



# Hygral and Thermal Expansion/Shrinkage Properties of Asbestos-Free Fibre Cement

S. A. S. Akers & M. Partl

Ametex AG, CH-8867 Niederurnen, Switzerland

(Received 17 February 1989; accepted 21 September 1989)

## Abstract

*This paper presents a study of basic properties of fibre cement composites related to expansion and shrinkage (thermal and hygral). It is aimed at providing a fundamental understanding of the material in order to describe its behaviour when exposed to natural weathering conditions. The migration of pore water and interrelated shrinkage stress of the products have been studied using model environmental chamber experiments. It is pointed out that movement of water within the product can be very complex and that a product exposed to the environment can experience complex stress concentrations depending on the density and/or pore size distributions and rate of absorption or loss of water. The build-up of stresses in aged products occurred at a slower rate than for non-aged products. Also the density of the product plays a very important role in the rate and build-up of stresses and this property appears to override the pore size distribution of certain composites.*

**Key words:** Fibre cement composites, cellulose fibres, synthetic fibres, thermal expansion, shrinkage, moisture content, composite materials, environmental tests, stresses, density, porosity, curing.

## INTRODUCTION

Cement-based composites exposed to natural weathering absorb water and may also give up water to their surroundings via a very complex inherent pore structure. The extent of pore water exchange and the speed at which it occurs depend on numerous factors, for example:

- the type of application (roofing or cladding);
- the shape of the product;

- the temperature of the surrounding environment;
- the relative humidity of the surrounding environment;
- rain, snow and ice conditions;
- wind velocity;
- the porosity and pore structure of the material;
- the orientation of the structure (anisotropy);
- the type of fibre in the product (cellulose or synthetic);
- the type of coating or impregnation applied to the product (coated on both sides and/or one side, edge coatings, etc.);
- the age of the material.

It is evident from the factors mentioned above that it would be an extremely difficult task (if not impossible) to describe or predict the exchange of water in the pores of a cement-based fibre composite during exposure to natural weathering. In fact much has been reported in the literature<sup>1-4</sup> regarding porosity and water absorption of cement pastes.

Although the transportation of pore water in a fibre cement composite is complex, it is important to describe in general terms the behaviour of a material under certain climatic conditions as the exchange of water in the pores results in dimensional changes (expansion or shrinkage) within the product. These changes would most certainly influence the behaviour of the product in its application. For example, a roofing slate is partly covered on its upper surface by a neighbouring slate and at the same time rests on slates below. When exposed to the elements only a portion of the upper surface of the slate is directly exposed to the natural environment. The portion of the slate in direct contact with the environment would obviously react differently from the covered portion or reverse side of the same slate. It is easy to

realise the very complex manner in which a slate could absorb or lose water. Further, because of the exchange of water through the pores of the slate, very complex stress fields are set up due to the non-uniform expansion and shrinkage. These stress patterns could result in complex deformations of the product and, in the extreme case, lead to localised cracking of the product. It is for this reason that the effect of water movement within the product should be studied. In addition, expansion and shrinkage of the product may also occur at varied temperatures which could be independent of the pore water. Temperature and humidity variations occur simultaneously during natural weathering and therefore both variables are to be superimposed when describing the behaviour of the material. This paper is concerned with fundamental studies aimed at a general understanding of the basic material properties which may be used for extrapolation purposes applied to the product under 'real' conditions.

## EXPERIMENTAL DETAILS

### Products

Fibre cement products were manufactured on a standard Hatschek machine used in the asbestos cement industry. The products manufactured and used for the studies described in this paper may be categorised as follows.

Product A — An autoclaved product (density  $1510 \text{ kg/m}^3$ ) containing 8% cellulose fibres, cement and silica (50:50).

Product B — A normally cured (ambient temperature and humidity) high-density ( $1870 \text{ kg/m}^3$ ) product containing 2% synthetic fibres, 4% cellulose fibres and cement.

Product C — A normally cured (ambient temperature and humidity), medium-density ( $1500 \text{ kg/m}^3$ ) product of similar mix formulation to product B.

Product D — A normally cured (ambient temperature and humidity), low-density ( $1230 \text{ kg/m}^3$ ) product of similar mix formulation to product B.

### Environmental chamber studies

The products were subjected to environmental chamber experiments in order to monitor their

expansion/shrinkage properties in varied climatic conditions. The environmental chamber used consisted of standard equipment manufactured by Köttermann capable of providing the varied climates required for the investigations described in this paper.

In order to obtain an insight into stresses which could be set up in a product during non-uniform shrinkage or expansion in natural weathering, model experiments were designed. Simple test apparatus designed for measuring restrained shrinkages was used (Fig. 1). The test comprised a tensile specimen,  $400 \text{ mm} \times 35 \text{ mm} \times 6 \text{ mm}$ , fixed between the jaws of a rigid steel frame with an attached cell used to measure tensile forces on the specimen during drying shrinkage. Shrinkage stresses were measured on the specimens fixed in the steel jaws of the restrained shrinkage frame. 'Actual' shrinkage was measured directly from an adjacent test specimen suspended freely in the chamber. The independent signals from the load cell and extensometer were recorded simultaneously with respect to time and stored on an IBM (PC-XT 286) computer. The stored data may be plotted in the form of stress versus time, and/or shrinkage versus time, curves.

Products were pre-conditioned by submerging them in water for 48 h at  $20^\circ\text{C}$  prior to the environmental chamber exposure. The specimens were fixed in the jaws of the restrained shrinkage equipment and exposed to an environment of  $20^\circ\text{C}$  at 95% RH for four days, after which the relative humidity was changed to 50%. The temperature was kept constant at  $20^\circ\text{C}$  throughout the exposure.

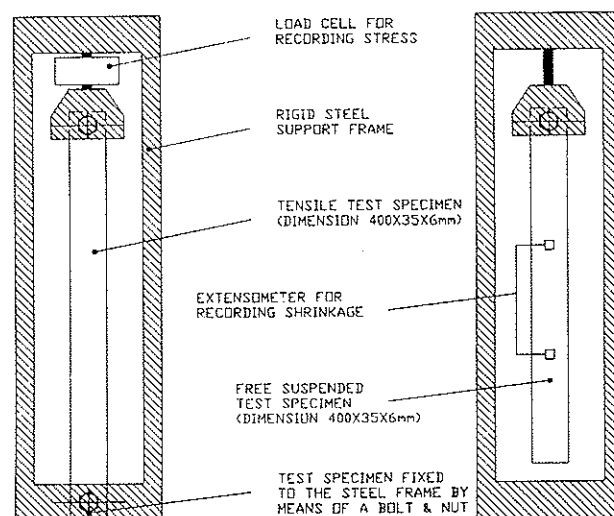


Fig. 1. Diagrammatic representation of equipment for restrained shrinkage measurements.

In order to study the influence of product age on restrained shrinkage, extreme laboratory-simulated experiments were conducted. For this particular study, products of similar mix formulation and density to Product C were used. The product had a history of five years' natural weathering exposure in Switzerland. For comparative purposes a non-aged equivalent was manufactured. The aim of the investigation was to assess the response of aged (naturally weathered) products to restrained shrinkage tests, and to compare these with the non-aged equivalent. An extreme laboratory exposure condition was chosen in order to test the limits of the stress build-up within aged and non-aged material. This test consisted of submerging the products in water for one week at 20°C and thereafter exposing them to an environment of 60°C and 10% RH.

In an additional investigation with different test equipment, the loss of water of the products was determined. For this purpose a water-saturated specimen (Product C) was suspended from a cantilever beam with a built-in load cell. In this way the loss of water from the pre-saturated specimen could be measured when it was exposed to varied climatic conditions. Climatic conditions consisted of 95% RH over a period of time and thereafter 50% RH. Temperature was kept constant at 20°C. The change in mass of the specimen was continuously plotted as a function of time. This value could be directly translated into moisture content of the specimen using the 'wet' and 'dry' mass values. Using the data obtained from restrained shrinkage specimens, the moisture content of the specimen could be plotted as a function of time and/or stress and/or shrinkage.

#### Determination of the coefficient of capillary water conductivity

In order to characterise varied materials according to rate of water absorption by the pores, the coefficient of capillary water conductivity was found to be a useful criterion. This can be determined by measuring the electrical conductivity, a method recently developed and successfully applied on concrete at the ETH Zurich.<sup>5</sup> The application of this method for fibre cement products is demonstrated here on the products A, B, C and D already described above.

The schematic representation given in Fig. 2 indicates several couples of silver electric contacts 10 mm wide which are attached on both sides of the specimens at a distance of 10 mm from each

other and parallel to the imposed humidity front. All sides of the specimens apart from the upper and lower edges were coated with a sealing varnish. The specimens were placed in a chamber having a high humidity (95%) and a temperature of  $20 \pm 5^\circ\text{C}$ . The uncoated lower edge of the specimen was submerged about 2 mm in water. The water penetrating from the lower edge causes a temporarily delayed change of the electrical conductivity  $L$  between the opposite electrodes. This conductivity is expressed as a function of  $t' = \sqrt{t}$  given in the equation:

$$\tau = \frac{\int_{L_0}^{L_w} t' dL}{\int_{L_0}^{L_w} dL}; t' = \sqrt{t}$$

where  $\tau$  represents the edge of a rectangle (Fig. 3) with length  $\Delta L$  which is equal in area to the horizontal integral of the conductivity curve. In order to calculate  $\tau$  for each pair of electrodes using the above equation it is useful to approximate the

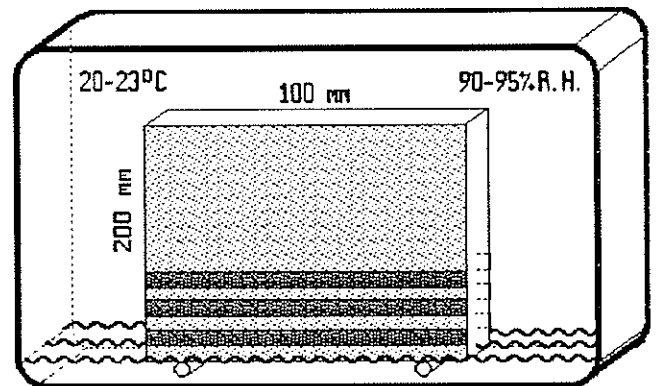


Fig. 2. Diagrammatic representation of equipment for water penetration measurements.

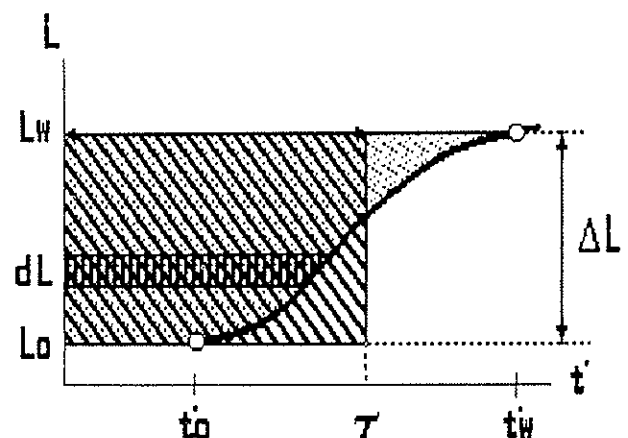


Fig. 3. Determination of the characteristic pressing time  $\tau$  from the electrical conductivity curve.

experimental curve  $L(t')$  to the maximum value of conductivity, i.e. in the range between  $t'_0$  and  $t'_w$ , using polynomial regression analysis. Hence the coefficient of capillary water conductivity is derived from the slope of the linear regression curve in the diagram where the contact times are plotted against the vertical position of the electrodes.

## RESULTS AND DISCUSSION

### Influence of ambient relative humidity

Stress/time and shrinkage/time curves obtained from restrained shrinkage and freely suspended specimens are given in Figs 4 and 5 respectively. The pre-conditioned ('wet') specimens were 99% water-saturated before they were placed in the environmental chamber. In a surrounding climate of 20°C and 95% RH, the water contained in the pores of the 'wet' products migrate into the surrounding environment and the product begins to 'dry out'. This results in 'drying' shrinkage which may be measured on the freely suspended specimen using an extensometer. Simultaneously, an associated strain may be measured on a specimen cut from the same product.

Comparing the various products tested (Fig. 4), it may be seen that the materials respond quite differently. For example, the autoclaved product (Product A) had a rapid stress build-up between 10 h and 20 h after which an equilibrium was achieved whereas the stress build-up in Product B remained increasingly progressive up to 72 h. The latter product did not achieve equilibrium at 72 h and was also at a lower stress level than Product A. The build-up of stresses in Products C and D was negligible at the start and only after 10 h and 30 h respectively could an increase in stress be detected. Very low stress levels were achieved in Product D even after 72 h. Changing the RH from 95% to 50% at constant temperature resulted in a further drying out of the products and in turn in more advanced shrinkage which led to increases in stress. It is again apparent that the build-up of stresses in Product A occurs at an increased rate and to greater stress levels than in other products tested.

The stress levels achieved by the various products throughout this experiment are well below the ultimate 'dry' tensile strengths (Table 1) and, in some products, are close to the 'wet' ultimate tensile strength value. The build-up of stresses in equivalent-density Products A and C does not

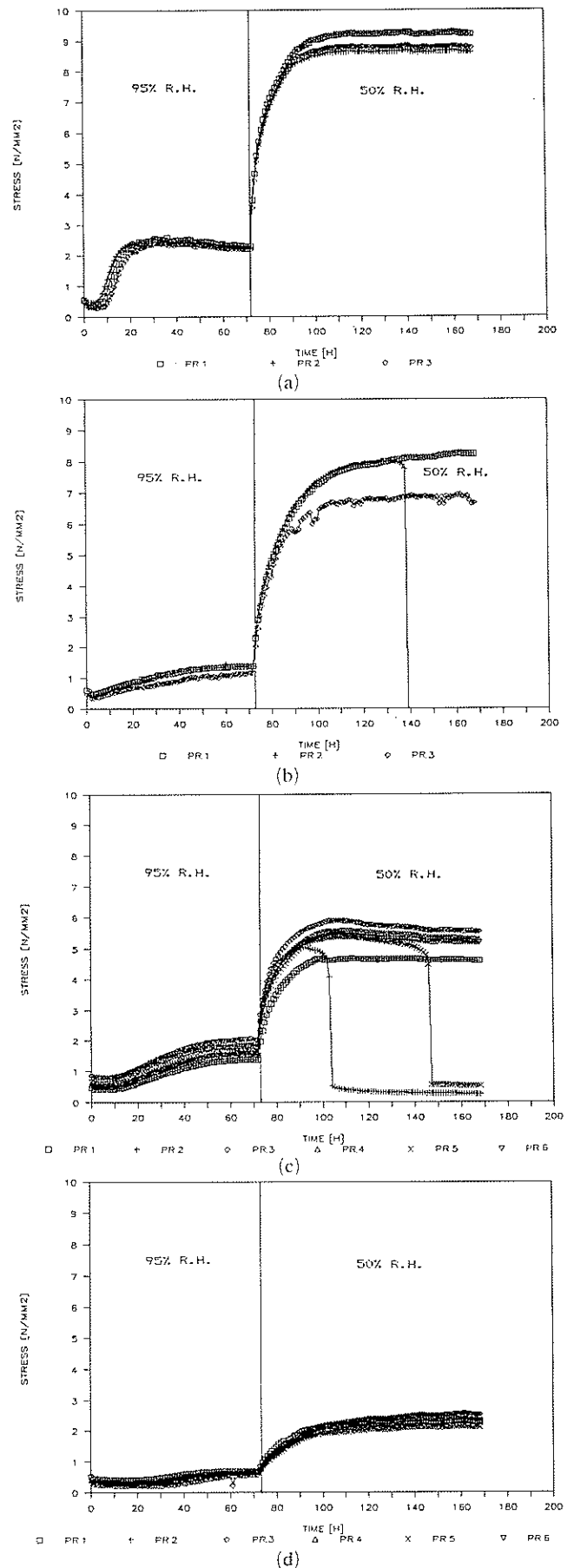


Fig. 4. Stress/time curves for tested products: (a) Product A; (b) Product B; (c) Product C; (d) Product D.

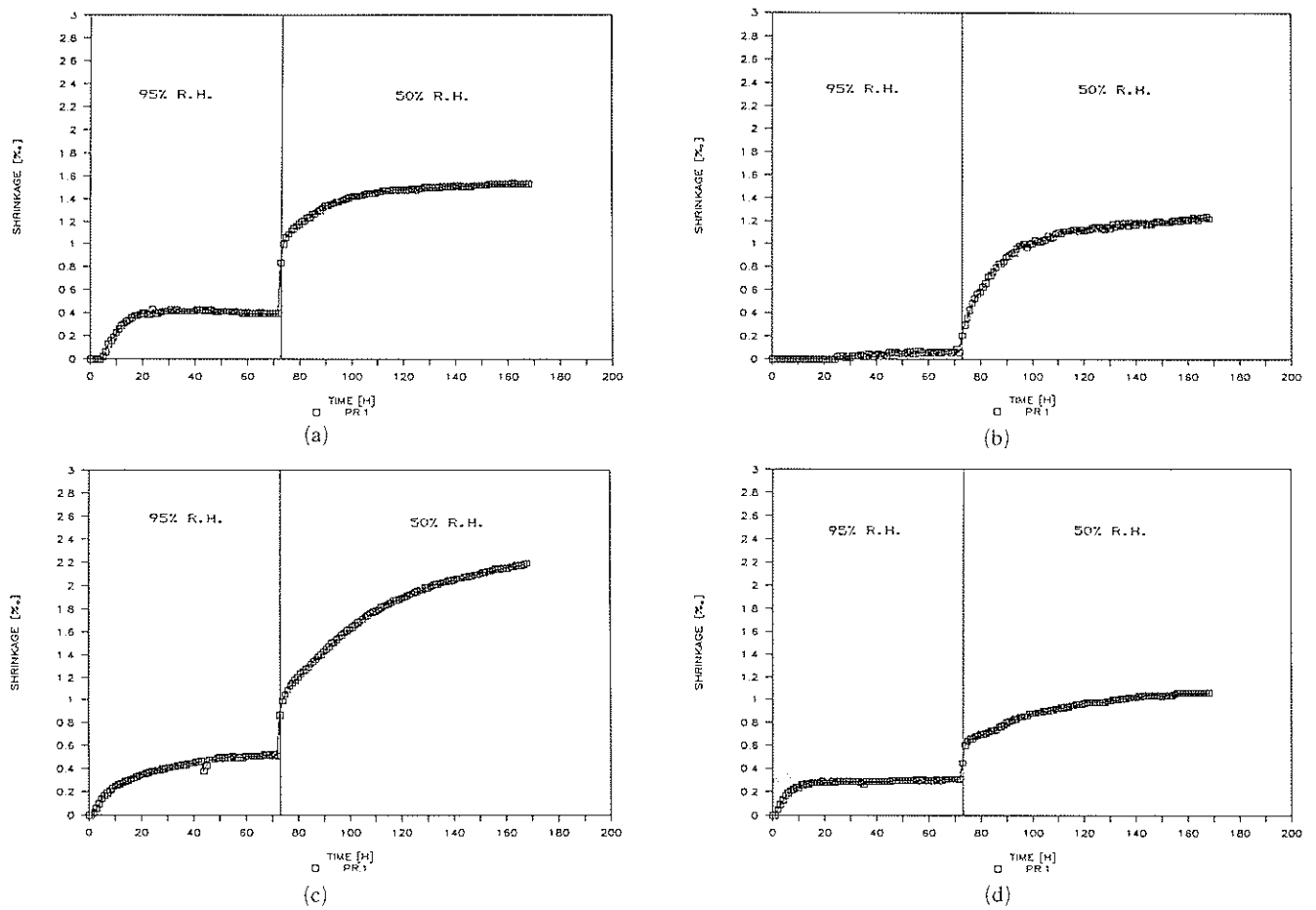


Fig. 5. Shrinkage/time curves for (a) Product A; (b) Product B; (c) Product C; (d) Product D.

Table 1. Properties of composites tested

Product	Tensile strength <sup>a</sup> (MPa)		Strain to failure (%)		Density (kg/m <sup>3</sup> )	Coeff. of capillary water conductivity (mm/h <sup>1/2</sup> )
	'Wet'	'Dry'	'Wet'	'Dry'		
A	9.2 ± 2.1	20.6 ± 0.8	0.28 ± 0.07	0.15 ± 0.01	1510 ± 10	9.2
B	9.0 ± 0.7	16.8 ± 1.2	0.09 ± 0.02	0.08 ± 0.01	1870 ± 10	4.19
C	7.0 ± 0.6	10.2 ± 1.7	0.11 ± 0.02	0.07 ± 0.03	1500 ± 20	10.15
D	3.8 ± 1.2	5.6 ± 1.3	0.25 ± 0.04	0.12 ± 0.03	1230 ± 10	31.97

<sup>a</sup>Tensile tests conducted on (a) 'Wet', water-saturated specimens submerged in a water bath for 48 h and (b) 'Dry', dried in an oven at 80°C for 48 h and subsequently tested at room temperature.

occur at an equivalent rate. It would appear, therefore, that the migration of the pore water of the products studied is rather complex, and not necessarily related to the density alone but also to other material properties as well.

#### Influence of product age

Products exposed to extreme laboratory-simulated conditions achieved shrinkage stresses exceeding the ultimate tensile strength of the products, thus resulting in failure of the product during the test. The results are given in Figs 6 and

7 for the non-aged and aged products respectively. The stress levels at failure for both aged and non-aged products were similar; however, the length of time to failure was significantly longer for the aged product. Also, the shrinkage value at ultimate failure for the aged product was significantly less. This is to be expected as the product becomes more rigid with age due to carbonation of the matrix, changing its pore structure. The slope of the curves confirms this.

The relevance of this type of test has been discussed earlier. Slates are exposed on the roof with

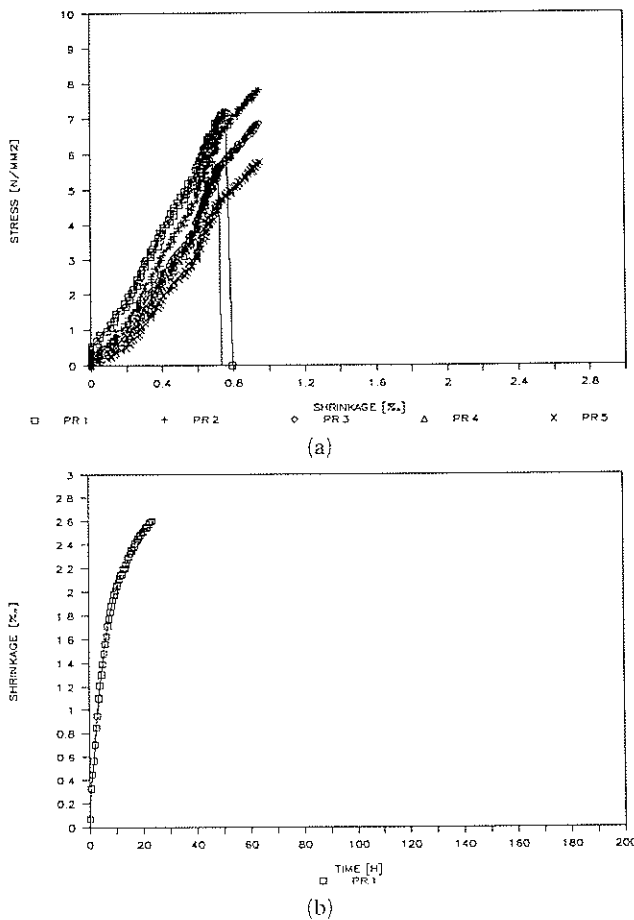


Fig. 6. Shrinkage effects of non-aged products subjected to 60°C and 10% RH.

a covered and uncovered (exposed) portion. The internal localised stress concentrations set up in the roofing slate during the drying out or wetting of the roof during weathering are transient and governed by the rate of water penetration as the material expands or shrinks. This would have an obvious influence on the intensity of the stress concentrations built up within the sheet and in turn could govern the propensity for cracking. As the rate of absorption for aged products is slower than that for the unaged equivalent, the stress concentrations between the covered and exposed portions of the slate could be smaller for aged products.

#### Influence of ambient relative humidity

From the curves given in Fig. 8, it may be seen that within 30 h the water content of Product C decreases from 26% to an equilibrium value of 18% under the climatic conditions of 95% RH and 20°C. However, this considerable loss of water leads to relatively small increases in stress due to the relatively small shrinkage occurring under these conditions. Changing the environ-

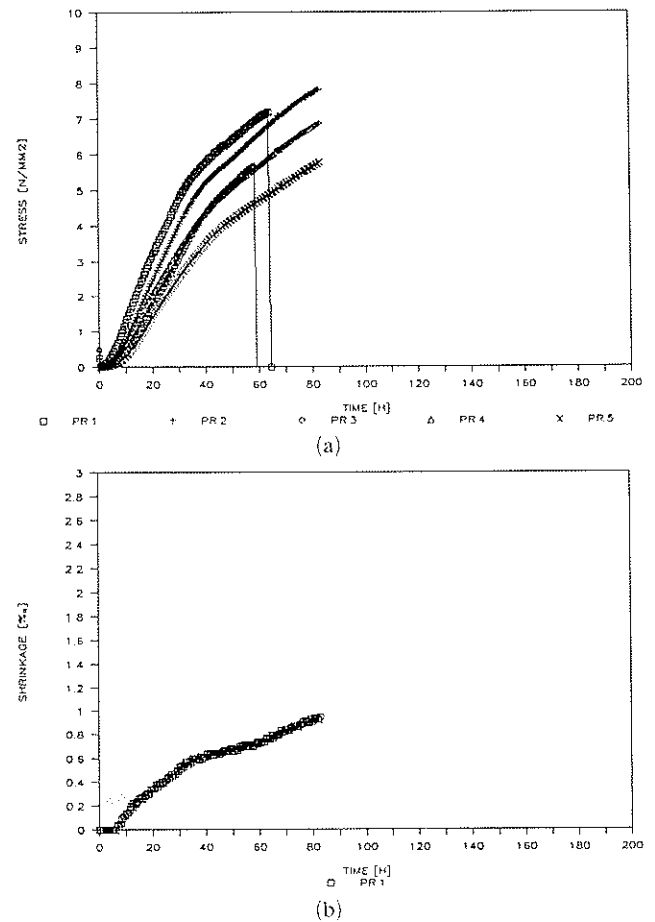


Fig. 7. Shrinkage effects of aged products subjected to 60°C and 10% RH.

mental conditions from 95% RH to 50% RH at constant temperature resulted in a further loss of water from 18% to 14% over a period of 30 h. Comparing the data obtained from this change in humidity with the previous conditions, a more significant increase in stress ( $\approx 4$  N/mm<sup>2</sup>) and shrinkage strain ( $\approx 1.6\%$ ) may be detected. Further, this occurred for a less significant loss of water (from 18% to 14%) compared with 26% and 18% under the former environmental conditions. This would suggest that a considerable loss of water is required in a product before significant shrinkage may occur. In other words, this could explain why some products only crack in extreme climatic variations and not in relatively mild climates.

#### Coefficient of capillary water conductivity

The results so far have dealt with water absorption or loss of water in all directions of the product. Fibre cement products manufactured on a standard Hatschek machine, however, have an anisotropic behaviour and the rate of exchange of

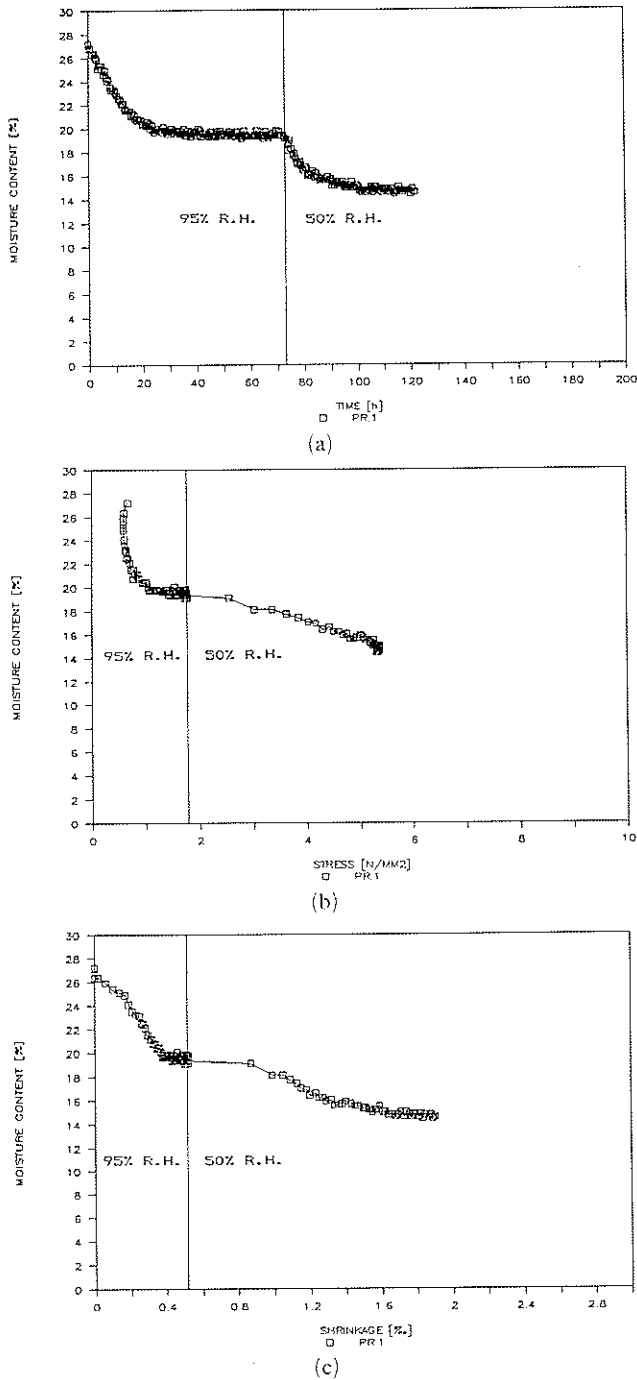


Fig. 8. Variation of water content with (a) time, (b) stress and (c) shrinkage strain for Product C.

water within the product could depend very significantly on the orientation of the product.

From a practical point of view, water penetration from the edges of a product exposed to natural weathering is an important factor to consider, particularly for roofs situated in alpine regions where damming up of water may take place under certain snow and ice conditions. To characterise the material behaviour in such situations, the coefficient of capillary water conductivity is appropriate.

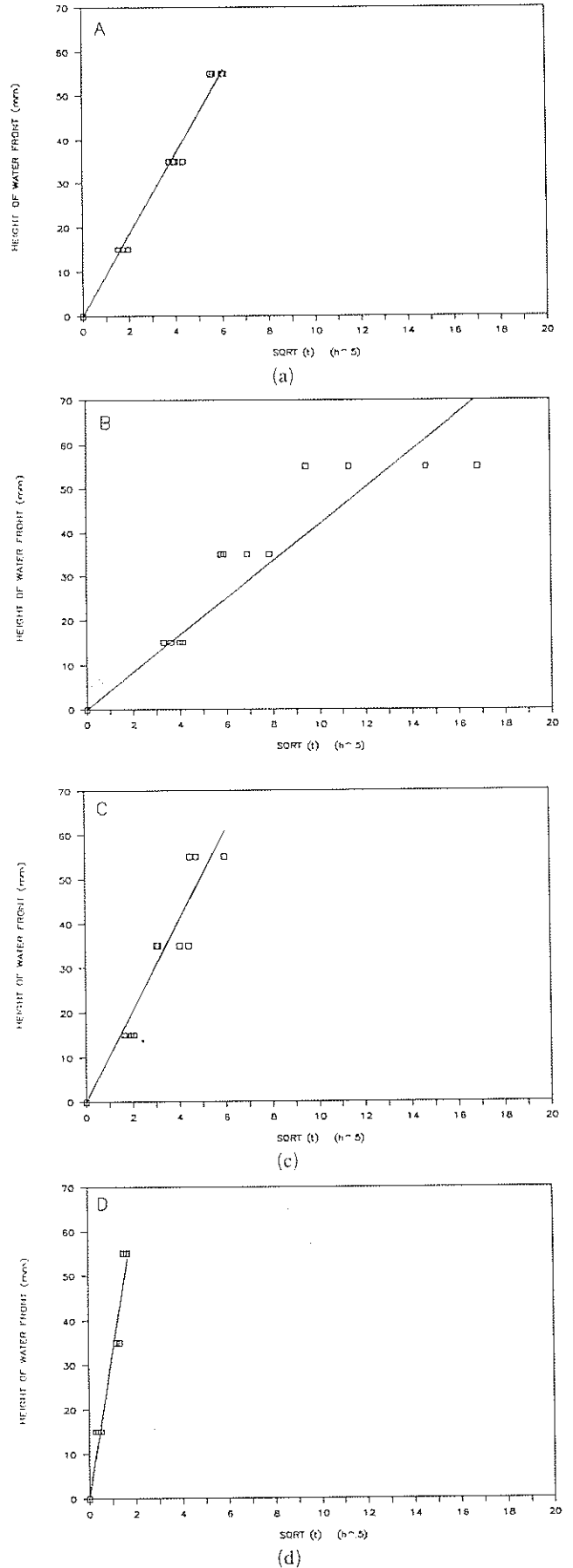


Fig. 9. Results of lateral water penetration tests for products (a) A, (b) B, (c) C, (d) D.

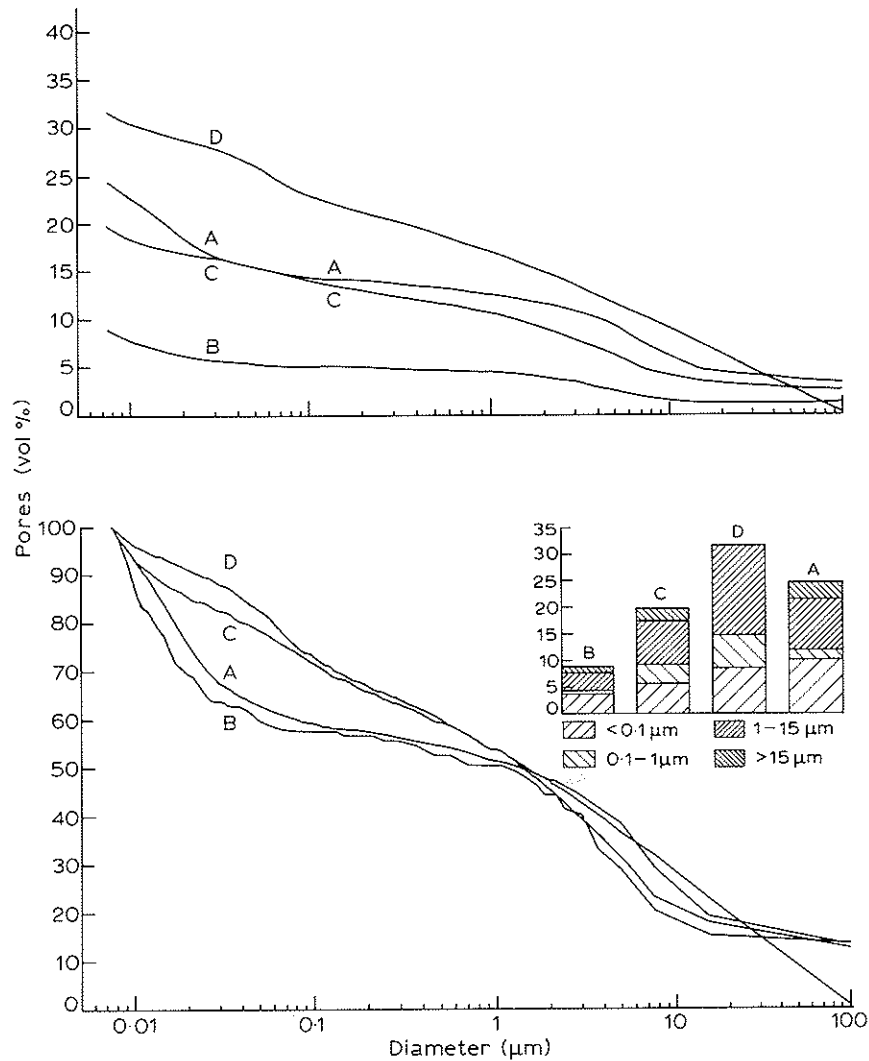


Fig. 10. Pore size distributions of Products A, B, C, and D.

Figure 9 shows the relation between the position of the electrodes and the contact time for Products A, B, C and D, and in Table 1 the coefficients of capillary water conductivity are given. It can be seen that for Product D, with the lowest density, the lateral water penetration occurs at the highest rate whereas the relatively dense Product B shows the smallest rate of absorption.

It is interesting that although Product A (autoclaved) is significantly different in mix formulations from Product C, which has an equivalent density, the absorption rates of both products are very similar. The results given in Fig. 10 shows that the pore size distribution (measured using standard mercury porosimetry equipment) of Product A is different from that of Product C. Thus it would appear that the density of the product is more important in influencing the rate of absorption than the pore structure.

## CONCLUDING REMARKS

1. Migration of the pore water of fibre cement products is complex and not entirely related to the density of the material; this has a significant influence on shrinkage properties.
2. Restrained shrinkage experiments have indicated that although the stress levels at failure between aged and non-aged products were similar, the rate of build-up of these stresses is much slower in aged products. Also, less shrinkage occurred in aged products.
3. A study of the migration of pore water within a product exposed to various environments has indicated that initial losses in pore water do not necessarily lead to greater internal stresses; more important are the rate at which the loss of water takes



place and its range within the product.

4. Density and porosity are related; however, for products of equivalent density having differing pore size distributions, the rate of absorption was similar. This would suggest that the density of the products, rather than the pore size distribution, dictates the absorption rate.

#### REFERENCES

1. Powers, T. C. & Brownyard, T. L., Studies of the physical properties of hardened portland cement paste. In *Proc. American Concrete Institute*, **43** (2) (October 1946) 101-31.
2. Goto, S. & Roy, D. M., The effect of W/C ratio and curing temperature on the permeability of hardened cement paste. *Cement and Concrete Research*, **11** (4) (July 1981) 575-9.
3. Relis, M. & Soroka, I., Limiting values for density and intrinsic shrinkage in hydrated portland cement. *Cement and Concrete Research*, **10** (4) (July 1980) 499-508.
4. Czernin, W., *Zementchemie für Bauingenieure*, Vol. 3, Berling-Bauverlag, Wiesbaden, 1977.
5. Peter, G., Yang, Q. & Rösli, A., 'Statistische Auswertung von Aufsaugversuchen an Beton zur Charakterisierung der schnellen Infiltration wässriger Lösungen', *Material und Technik*, **14** (1) (March 1986) 13-27.